Multi degree-of-freedom position sensing by combination of laser speckle correlation and range-resolved interferometry

Thomas O.H. Charrett[*], Thomas Kissinger and Ralph P. Tatam
Engineering Photonics, Cranfield University, MK43 0AL, UK.

ABSTRACT

This paper reports on the development of an end-effector mounted, multi degree-of-freedom positioning sensor capable of measuring the (x,y,z) movements relative to an object. The instrument termed wPOS (workpiece Positioning Sensor), combines two complimentary non-contact optical techniques; laser speckle correlation (LSC) and Range-Resolved Interferometry (RRI). Laser speckle correlation is used to measure the in-plane position (x,y) relative to a reference point, while the RRI system provides an out-of-plane (z) absolute range measurement and correction of the in-plane LSC measurement for varying working distance. The concept and operating principles of the instrument is described along with details of the prototype sensor implementation and exemplar results showing accuracies of <30µm after 0.75m lateral travel and repeatability between measurements of ~7 µm.

Keywords: Laser speckle; Interferometry; Range Resolved Interferometry; Displacement sensing; Positioning; Tool path; Tool speed;

1. INTRODUCTION

The use of industrial robotics offers increased flexibility and lower costs when compared with expensive Computer Numerical Control (CNC) Cartesian systems, however for many manufacturing applications they lack the positioning accuracy required. Industrial robots are more prone to disturbances from process and environmental forces due to the comparatively low mechanical stiffness of typical industrial robots[1,2]. Additionally, there can be significant deviations from the desired tool-path and tool-speed that are not captured by the kinematic models used to convert joint encoder positions to Cartesian end-effector position. Geometrical errors from manufacturing, machining tolerances, and the assembly of the robot components will propagate to a combined inaccuracy in the robots pose (position and orientation)[2] as will environmental factors such as temperature changes that lead to distortions of the robot, and are hard to predict[3]. The result is that typical industrial robots offer highly repeatable motion but the positioning accuracy can be relatively low. For example Morozov *et al*. investigated the positioning accuracy (point-to-point movement) and continuous path accuracy using a Kuka KR5 robot and a Leica AT901-LR laser tracker[4]. They found typical positional accuracies of 0.8mm and repeatability of 70µm, however at points in the robots work envelope this was up to 1.3mm with 120µm. For continuous operations where it is desirable to have the robot follow a precise path, the performance can be much worse, with the path accuracy (as defined by ISO 9283:1998 as the maximum perpendicular distance from the path) measured[4] to be between 1.8 and 4.5mm .

The ability to determine the robots position and characterize robot motion is therefore of great interest in many manufacturing operations where these positioning errors are critical for process quality, for example, in many continuous machining operations the feed rate or tool speed is critical to ensure process quality[5]. In other contact tasks, such as polishing and drilling, the comparatively low mechanical stiffness of typical industrial robots can result in excessive tool slippage and vibration resulting in errors in dimension and/or poor surface quality, with deflections of up to 0.25mm reported in robotic milling operations[6] and in robotic additive manufacturing tool speed variations can lead to excessive material deposition[7].

To provide feedback and correct for these errors improved sensors and instrumentation are required. External measurements systems such as laser trackers[8], light or radio based beacon systems such as iGPS [9,10] can be used to track the motion of the robot end-effector. However these are expensive and suffer limitations; laser trackers need to be mounted externally to the robot and maintain a continuous line of sight, while iGPS systems have been shown to improve the positioning accuracy from 4.53mm to 0.38mm this does not yet meet the desired 0.2mm[10]. Lower cost

---

[*] t.charrett@cranfield.ac.uk

approaches using position sensitive detectors[11] or vision systems[12,13] have been proposed but are limited in operating space or update rates. In this paper we report the development of an end-effector mounted, multi degree-of-freedom positioning sensor capable of measuring the (x,y,z) movements relative to the workpiece. The instrument, termed wPOS (workpiece Positioning Sensor), combines two complimentary non-contact optical techniques; laser speckle correlation (LSC) [2, 3] and Range-Resolved Interferometry (RRI) [4]. Laser speckle correlation is used to measure the in-plane position (x,y) relative to a reference point, while the RRI system provides an out-of-plane (z) absolute range measurement. In the following sections we outline the concept and operating principles of the instrument (section 2) and present details of the prototype sensor implementation (section 3) and exemplar results (section 4).

2. CONCEPT & OPERATING PRINCIPLES

The concept of the wPOS instrument is shown in figure 1 where a sensor head is attached to the robot end-effector and continually measures/tracks the position of relative to the workpiece. The Range-Resolved Interferometry (RRI) sub-system allows the measurement of the out-of-plane motion while Laser Speckle Correlation (LSC) is used for the measurement of the in-plane motion (x,y).
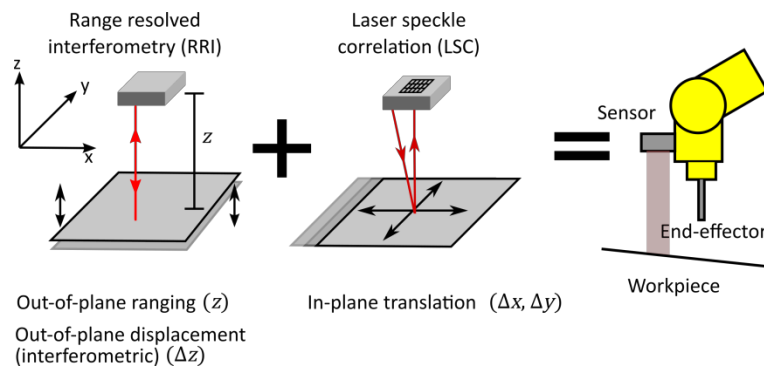

Figure 1. Operating concept of the wPOS instrument combining Range Resolved Interferometry (RRI) and Laser Speckle Correlation sensing (LSC)

Range-resolved interferometry (RRI)[14] is a cost-effective interferometry technique based on the sinusoidal wavelength modulation of widely available and robust telecoms laser diodes. This allows high-quality measurement of the interferometric phase giving typically nm level resolution in displacement measurements at multi-kHz bandwidths. In common with other interferometric methods this allows only relative displacement measurements referenced to a starting position and not the absolute range. However the range-resolving properties of the technique enables discrimination between signals originating at different ranges and this allows the additional lower-resolution measurement of the absolute distance at typically 10 to 100 µm resolution.

The principle is shown in Figure 2, where in a) a conceptual interferometer is shown with two semi-transparent objects located at different optical paths differences (OPDs). In Figure 2, b) and c) the resulting phase modulation and photo-detector signals that would be recorded are shown for the two objects individually. The combined photo-detector signal resulting from the two objects in the beam in Figure 2 a) is shown in Figure 2 d), together with a periodic window function applied before signal demodulation. For each OPD position, the RRI demodulation algorithm then uses a calculated using time-variant complex carrier signals calculated for different OPDs. The signal amplitude resulting from this demodulation as a function of OPD is shown in Figure 2 e). Further details of the RRI signal processing can be found in Kissinger *et al.*[14]. In practice the interferometer is constructed using standard telecoms industry laser diodes and optical fiber components, with the interferometers formed between the fiber tip reflections and the object(s), as shown in Figure 2 f) and the signal processing and modulation control implemented using a field programmable gate array (FPGA). To obtain absolute distance measurements the return signal strength, Figure 2 e) is evaluated as a function of range using a Gaussian peak fit, while interferometric displacement measurements of individual targets at nanometer resolutions are also possible by applying quadrature demodulation at a single OPD to obtain interferometric phase information[14].
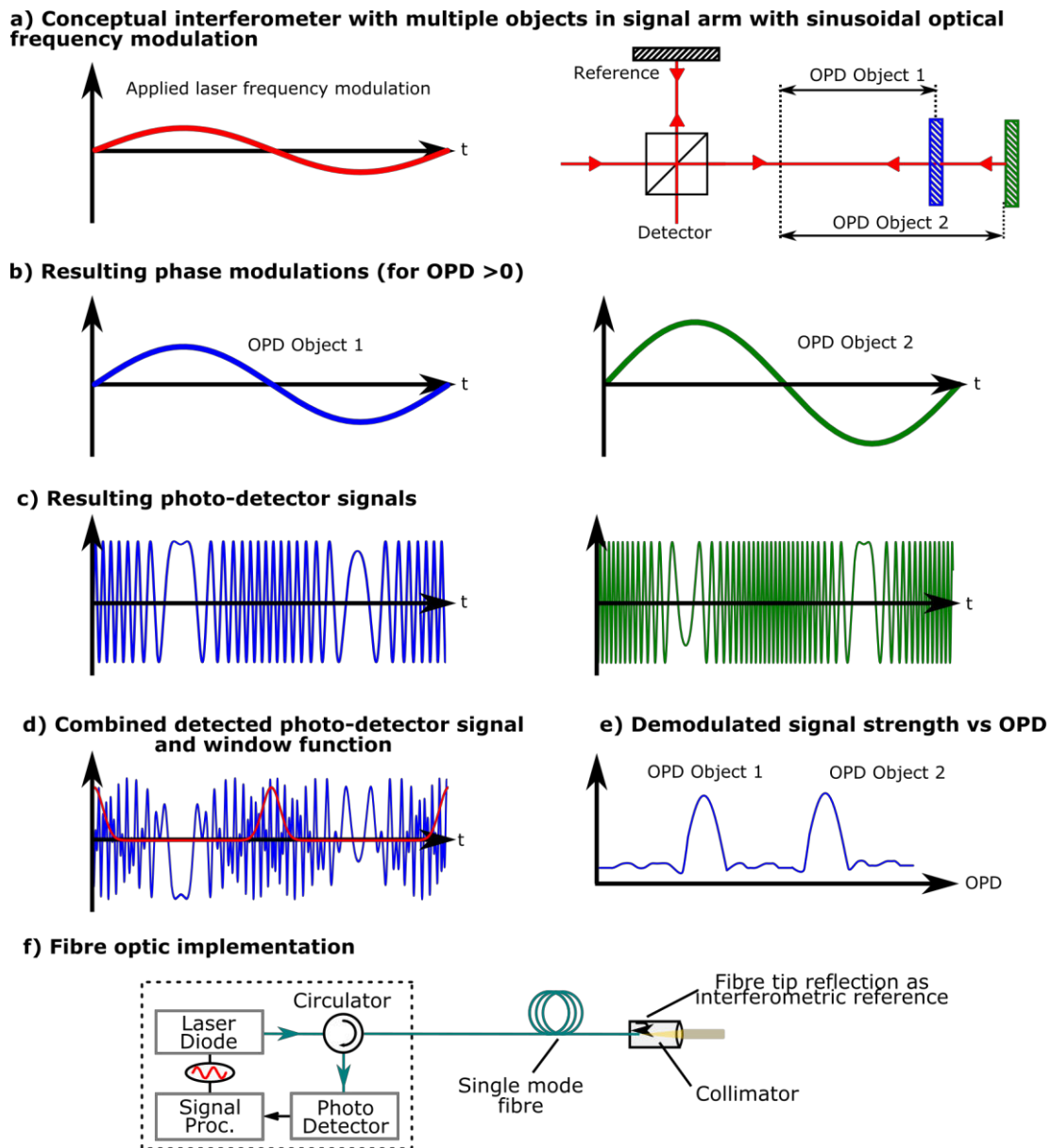
a) Conceptual interferometer with multiple objects in signal arm with sinusoidal optical frequency modulation

Applied laser frequency modulation

Reference

OPD Object 1

Detector

OPD Object 2

b) Resulting phase modulations (for OPD >0)

OPD Object 1

OPD Object 2

c) Resulting photo-detector signals

d) Combined detected photo-detector signal and window function

e) Demodulated signal strength vs OPD

OPD Object 1

OPD Object 2

OPD

f) Fibre optic implementation

Laser Diode

Circulator

Fibre tip reflection as Interferometric reference

Signal Proc.

Photo Detector

Single mode fibre

Collimator

Figure 2 – The RRI concept; in a) a conceptual interferometer is shown with two semi-transparent objects at different optical path differences (OPD), sinusoidal optical frequency modulation is applied to the laser and the resulting phase modulations b) and photo-detector signals c) are shown for the two objects individually. In d) the resulting combined photo-detector signal is shown together with the Gaussian window function applied before demodulation. The signal amplitude resulting from demodulation at different OPDs is shown in e) with two peaks yielding the object ranges. Finally, in f) a fiber optic implementation of the interferometer is shown.

The in-plane positioning is achieved by the use of high-speed laser speckle correlation (LSC)[15–17]. The concept of this approach is simple, the workpiece surface is illuminated with a laser source and the resulting scattered light pattern recorded by a camera. No imaging lens is necessary; rather the camera is used as an array detector to sample the resulting scattered light field – the objective laser speckle pattern and laser speckle patterns can be formed from a wide variety of surfaces as long as the surface is rough at the scale of the optical wavelength ($\sim$0.5 - 0.7µm), i.e. any diffusely reflecting surface including a wide variety of surfaces such metal, paper, sand and rocks[18]. Figure 3 illustrates the signal processing principle used which consists of tracking the translation of the acquired speckle pattern at high speed (~500fps) via the application of the two-dimensional normalized cross-correlation[19]. The offset of the peak from the center of the

correlation image yields the shift of the speckle pattern, (A_x, A_y) which can then be related to the x and y translations between the sensor and workpiece occurring between the images via geometry dependent scaling factors[20] that relate the object motion (a_x, a_y, a_z) to the speckle shift (A_x, A_y). Finally the peak location is compared to the reference image bounds to ensure that the reference and live images overlap, with the current image stored as the new reference and the reference position updated, when the shift is close to exceeding the maximum allowable shift.
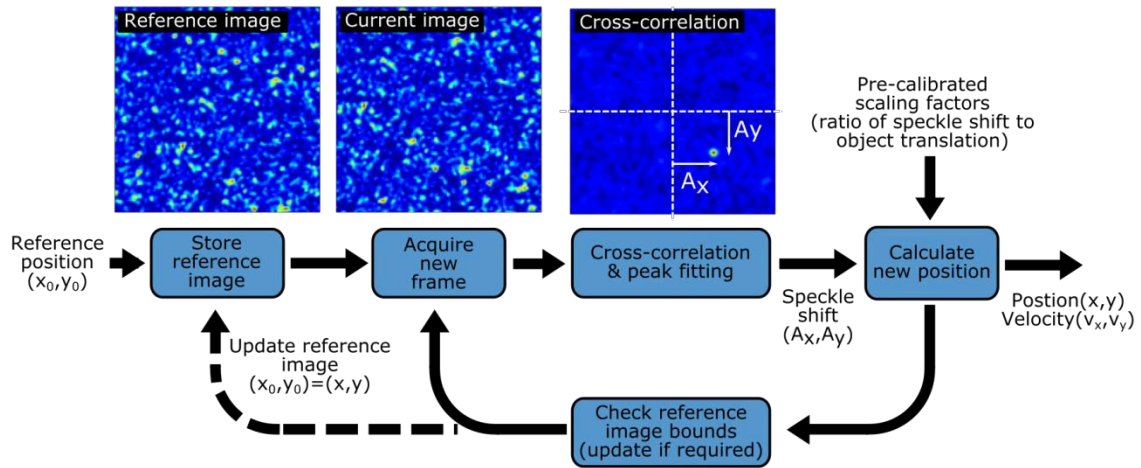

Figure 3. Laser speckle correlation concept. From left to right; a reference speckle image is acquired at the starting position, newly acquired speckle images are then captured, processed via 2D normalized cross-correlation and peak fitting to find the the shift between the two patterns (A_x, A_y). The new position and velocity is then calculated using pre-calibrated scaling factors. Finally the peak location is compared to the reference image bounds with the current frame stored as the new reference when the patterns is close to exceeding the maximum allowable shift.

3. COMBINED INSTRUMENT

The combined wPOS instrument is shown in Figure 4 a) and consists of a 19 inch rack mounted signal processing unit with armored optical fiber delivery to the sensor head shown in Figure 4 b). The signal processing unit contains a personal computer for control and processing together with the RRI sub-system and LSC laser and power supplies. The RRI sub-system consisted of a 1550nm fiber coupled telecoms diode (Eblana photonics, EP1550-0-NLW, 3.4mW average power output) together with an FPGA and high-speed digital-to-analogue convertor (DAC) for modulation of the RRI laser together with an InGaAS photodetector (Thorlabs PDA05CF2) and 100 MHz analogue-to-digital convertor (ADC) for detection. The LSC laser was a 658nm fibre-coupled laser diode (Blue Sky Research, FibreTec II FTEC2658-P60PA0) , max output 60 mW, operating output 0.6 mW). This is a temperature stabilized diode operating in constant current mode to prevent changes to the output wavelength that could appear as a translation of the speckle pattern. The LSC processing was performed on the control PC integrated into the wPOS instrument.

The sensor head, shown in Figure 4 b), was a custom designed 3D printed mount containing focusing/collimation lenses for both RRI illumination and light collection (@ 1550nm), a focusing lens for LSC illumination (@658nm) and a high speed USB3 camera (Ximea MQ013RG-ON) and laser line optical filter to record the laser speckle patterns. The sensor head is connected via armored optical fiber and camera lead to a control and signal processing unit located remotely.
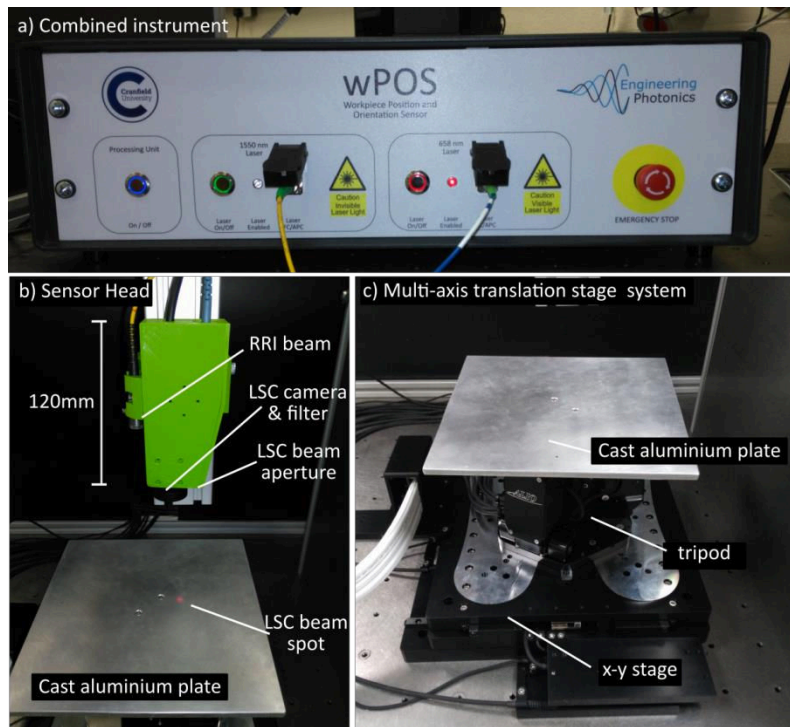
Figure 4 – a) Photograph of wPOS instrument and b) prototype sensor head and c) multi-axis translation stage used for calibration and testing.

The signal processing for the RRI and LSC are performed separately in real time on the control PC, with range values being streamed from RRI process to the LSC process via a TCP/IP network socket connection. The RRI sinusoidal modulation and data rate is 49 kHz however this is down-sampled to 1.5 kHz for peak fitting when determining the range. The LSC sensor is calibrated at a number of different working heights measured using the RRI system, and covering the expected range of operation, typically between ±5mm from the designed working distance. At each working height the scaling factors are measured by the application of repeated controlled displacements in both x and y directions independently using a high-accuracy translation stage. In measurements, the LSC processing proceeds as shown in Figure 3 starting from an initial reference position. As each new camera frame is acquired the average of the sixteen most recently acquired RRI range measurements is used to determine the correct scaling factors by linear interpolation between calibration values. The calculated (x,y,z) values are then streamed via a second TCP/IP network connection to a client PC/laptop for data display and storage.

4. RESULTS

The accuracy and repeatability of the system have been assessed using a laboratory trial where the sensor was mounted above a cast aluminium tooling plate attached to a 6 degree-of-freedom positioning stage (ALIO Hybrid-Hexapod AI-HYBRID-HEX-60XY-15Z-56R) as shown in Figure 4 b) and c). This allowed controlled x and y translations at velocities up to 500mm/s with a translational accuracy of <4 µm and repeatability <3µm together with the ability to adjust the working height via the tripod. A rectangular path of 175 x 200 mm (total travel = 0.75m) was traversed with an artificial 1mm height change between two sides of the rectangle. This path was then repeated multiple times to allow a preliminary assessment of the accuracy and repeatability of the measurements for different motions.

The results shown in Figure 5 a) show the path with the height change applied as a 1mm step, with multiple consecutive measurements of the same path represented by the different colours overlaid. Figure 5 b) shows an enlarged region of ±30µm area around the origin with the same data. It can also be seen that the sensor repeatability is high with consecutive measurements overlaid to with ~5 µm. The accuracy can be assessed by comparing the offset between the

(0,0) mm starting position and the calculated position after the stage has returned to this point. The initial starting position can be seen by the cluster of points around the origin in Figure 5 b), corresponding to vibrations when the stage was at rest. The motion then proceeds in the positive x direction and the returning path is then shown entering from the top before coming to a rest at a final calculated position offset by < 15µm from the origin. As the LSC approach relies on continuously tracking the position the overall accuracy will depend upon the distance traveled, with this result corresponding to an accuracy of ~20µm/m travel.

The performance is slightly worse if the range change is applied in a continuous gradient, Figure 5 c) & d), with the accuracy now <30µm after 0.75m travel and the repeatability ~7 µm. This may be due to the offset between the RRI measurement beam and the LSC measurement spot of ~20mm, if there is any difference in the surface range between these two measurements points this will introduce errors in the scaling factors used in the calculation of the in-plane position resulting in increased positioning bias errors. This will be addressed in future implements using collinear RRI and LSC beams to ensure surface range and hence LSC scaling factors are determined at the same point.
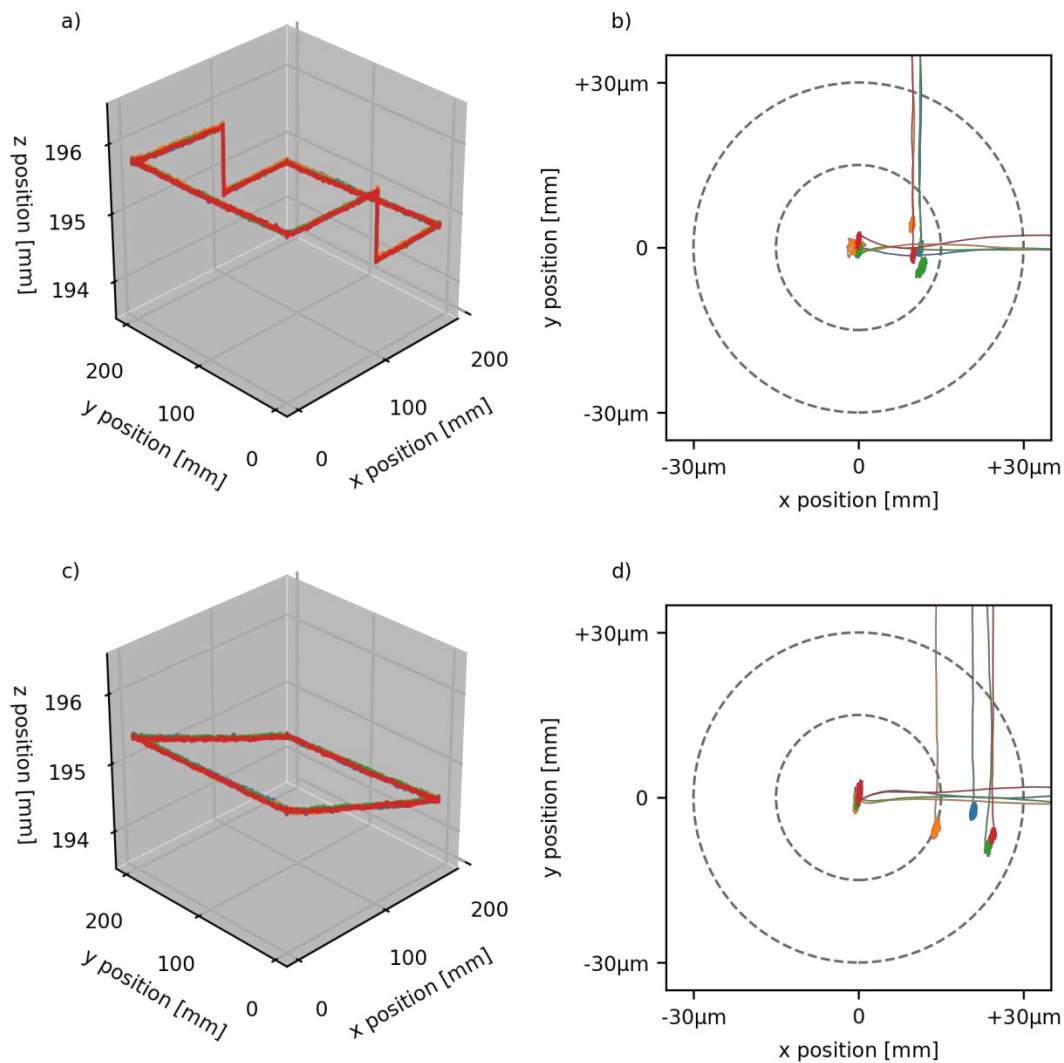

Figure 5 – 3D position measurements for a rectangular path with a 1mm height change between two-sides for a) & b) a step change and c) & d) a gradient change, here multiple measurements are overlaid showing repeatability of the robot path and sensor. Parts b) and c) show enlarged views of the *x,y* axis in around the origin (initial & final position) showing the offset error in the final measured position, with the overlaid circles showing the 15um and 30um error bands.

5. CONCLUSIONS

In this paper we have presented the combination of two measurement techniques, Range Resolved Interferometry (RRI) and Laser Speckle Correlation (LSC) to enable three-dimensional robot positioning relative to the workpiece via an end-effector mounted sensor. Out-of-plane range measurements are available at 1.5 kHz using the RRI technique and in-plane LSC measurements are made at 500 Hz. The RRI range measurements are applied to calculate the scaling factors used in converting from speckle translation to sensor translation and correct for any working distance variations. Initial results suggest that measurement accuracies of ~40µm/m travel should be achievable, with repeatability of ~5 µm.

An improved sensor head with the RRI and LSC laser beams collinear is proposed to avoid increased errors resulting from measurement of the range at an offset from the LSC measurement point and a full characterization of the measurement accuracy and precision is planned over a wider range of x,y,z motions and larger travel ranges.

ACKNOWLEDGEMENTS

REFERENCES

[1] Brogårdh, T., "Present and future robot control development - An industrial perspective," Annu. Rev. Control 31(1), 69–79 (2007).

[2] Schneider, U., Ansaloni, M., Drust, M., Leali, F. and Verl, A., "Experimental Investigation of Sources of Error in Robot Machining," [Communications in Computer and Information Science], 14–26 (2013).

[3] Heisel, U., Richter, F. and Wurst, K.-H., "Thermal Behaviour of Industrial Robots and Possibilities for Error Compensation," CIRP Ann. 46(1), 283–286 (2007).

[4] Morozov, M., Riise, J., Summan, R., Pierce, S. G., Mineo, C., MacLeod, C. N. and Brown, R. H., "Assessing the accuracy of industrial robots through metrology for the enhancement of automated non-destructive testing," IEEE Int. Conf. Multisens. Fusion Integr. Intell. Syst., 335–340 (2017).

[5] Chen, Y. and Dong, F., "Robot machining: Recent development and future research issues," Int. J. Adv. Manuf. Technol. 66(9–12), 1489–1497 (2013).

[6] Bauer, J., Friedmann, M. and Hemker, T., "Analysis of Industrial Robot Structure and Milling Process Interaction for Path Manipulation," [Process Machine Interactions], B. Denkena and F. Hollmann, Eds., Springer Berlin Heidelberg, Berlin, Heidelberg, 245–263 (2013).

[7] Bandari, Y. K., Charrett, T. O. H., Michel, F., Ding, J., Williams, S. W. and Tatam, R. P., "Compensation strategies for robotic motion errors for additive manufacturing (AM)," Int. Solid Free. Fabr. Symp., Austin, Texas (2016).

[8] Gharaaty, S., Shu, T., Xie, W. F., Joubair, A. and Bonev, I. A., "Accuracy enhancement of industrial robots by on-line pose correction," 2017 2nd Asia-Pacific Conf. Intell. Robot Syst. ACIRS 2017 (2017).

[9] Wang, Z., Mastrogiacomo, L., Franceschini, F. and Maropoulos, P., "Experimental comparison of dynamic tracking performance of iGPS and laser tracker," Int. J. Adv. Manuf. Technol. 56(1–4), 205–213 (2011).

[10] Trabasso, L. G., Santos, K. M., Suterio, R., Villani, E., Apetz, J. and Mosqueira, G., "Analysis of the indoor GPS system as feedback for the robotic alignment of fuselages using laser radar measurements as comparison," Robot. Comput. Integr. Manuf. 28(6), 700–709 (2012).

[11] Wang, C., Chen, W. and Tomizuka, M., "Robot end-effector sensing with position sensitive detector and inertial sensors," 2012 IEEE Int. Conf. Robot. Autom., 5252–5257 (2012).

[12] Du, G., Shao, H., Chen, Y., Zhang, P. and Liu, X., "An online method for serial robot self-calibration with CMAC and UKF," Robot. Comput. Integr. Manuf. 42, 39–48 (2016).

[13] Pérez, L., Rodríguez, Í., Rodríguez, N., Usamentiaga, R. and García, D., "Robot Guidance Using Machine Vision Techniques in Industrial Environments: A Comparative Review," Sensors 16(3), 335 (2016).

[14] Kissinger, T., Charrett, T. O. H. and Tatam, R. P., "Range-resolved interferometric signal processing using sinusoidal optical frequency modulation," Opt. Express 23(7), 9415–9431 (2015).

[15] Yamaguchi, I., "Speckle Displacement and Decorrelation in the Diffraction and Image Fields for Small Object Deformation," Opt. Acta Int. J. Opt. 28(10), 1359–1376 (1981).

[16] Charrett, T. O. H., Bandari, Y. K., Michel, F., Ding, J., Williams, S. W. and Tatam, R. P., "A non-contact laser speckle sensor for the measurement of robotic tool speed," Robot. Comput. Integr. Manuf. 53(April), 187–196 (2018).

[17] Charrett, T. O. H., Bandari, Y. K., Michel, F., Ding, J., Williams, S. W. and Tatam, R. P., "Laser speckle velocimetry for robot manufacturing," Proc SPIE Opt. Meas. Syst. Ind. Insp. X 10329, P. Lehmann, W. Osten, and A. Albertazzi Gonçalves, Eds., 103291Z, Munich (2017).

[18] Charrett, T. O. H., Waugh, L. and Tatam, R. P., "Speckle velocimetry for high accuracy odometry for a Mars exploration rover," Meas. Sci. Technol. 21(2), 025301 (2010).

[19] Lewis, J. P., "Fast normalized cross-correlation," Vis. interface 10(1), 120–123 (1995).

[20] Charrett, T. O. H. and Tatam, R. P., "Objective speckle displacement: an extended theory for the small deformation of shaped objects," Opt. Express 22(21), 25466 (2014).

School of Aerospace, Transport and Manufacturing (SATM)   Staff publications (SATM)

2019-06-21

Multi degree-of-freedom position sensing by combination of laser speckle correlation and range-resolved interferometry

Charrett, Thomas O. H.